ON/OFF Spiroconjugation through Peripheral Functionalization: Impact on the Reactivity and Chiroptical Properties of Spirobifluorenes

Ani Ozcelik+,[a] Daniel Aranda+,[b] Raquel Pereira-Cameselle,[a] María Talavera,[c] Berta Covelo,[d] Fabrizio Santoro,*[b] Ángeles Peña-Gallego,*[e] and J. Lorenzo Alonso-Gómez*[a]

In memory of Prof. Dr. François Diederich

Spirobifluorenes are an important class of spiro compounds frequently used in the field of organic electronics. However, harnessing spiroconjugation to obtain high-performance in such structural motifs remains unexplored. We herein propose that peripheral functionalization may serve as a useful tool to control spiroconjugation in an ON/OFF manner on both chemical reactivity and photophysical properties. In particular, the ratio of mono- and di-functionalized spirobifluorenes found experimentally during their synthesis were found to be 3/2, 7/2, and 12/2 for phenyl, nitro-phenyl and amino-phenyl analogues, respectively. These remarkable reactivity differences correlate with the spiroconjugation character evaluated theoretically at the CAM-B3LYP/6-31G(d,p) level of theory. Additionally, comparison of experimental and predicted optical and chiroptical responses shows that spiroconjugated molecular orbitals have a significant or negligible involvement on the main electronic transitions depending on the peripheral functionality of the spirobifluorene.

Introduction

The discovery of spiroconjugation can be traced back to 1967.[1,2] It arises from through-space orbital interactions between two π-systems that are orthogonally linked by a common tetrahedral atom.[3,4] In such a spiro arrangement, stabilized spiro-bonding and destabilized spiro-antibonding molecular orbitals (MOs) are formed, if p orbitals embrace appropriately. The energy difference between spiro-antibonding and spiro-bonding MOs is referred to as spiro-splitting (ΔE_s) and it is explained in terms of matching and mismatching combinations of the p orbitals in space.[5] Several studies have provided theoretical[1,2,6–8] and experimental evidence on spiro-conjugation by π-facial selectivity in Diels–Alder reactions of spiro-linked dienes[9,10] or by employing spectroscopic tools including UV/Vis[11] and photoelectron spectroscopies,[3,5,12–14] among others.[15] However, strategies for conscious tailoring and implementation of spiroconjugation into functional materials or even simple chromophoric systems are currently not available. Effective concepts to control spiroconjugation along with spiro systems that are easy to access, substitute, and thoroughly analyzed would boost the performance of functional materials.

Spirobifluorenes (SBFs) constitute an important class of spiro compounds, in which fluorene rings are orthogonally fused through a spiro carbon atom. SBFs offer high solubility and spiroconjugation,[16,17] and the 90° arrangement of the two fluorene rings around the spiro carbon leads to a rigid 3D structure and high stability. Given all these features, SBFs have found many applications in organic electronics,[18–20] catalysis,[21] and polymer chemistry.[22–24] The expression of spiroconjugation in SBFs stems from the fully antisymmetric combination (AA) between four p orbitals of the carbon atoms directly attached to the spiro center with respect to the two perpendicular planes (Figure 1). The HOMO of the fluorene subunits of SBF splits into spiro-antibonding HOMO and spiro-bonding HOMO-1 as a

[a] Dr. A. Ozcelik,+ Dr. R. Pereira-Cameselle, Dr. J. L. Alonso-Gómez
Departamento de Química Orgánica
Universidad de Vigo
Campus Universitario, 36310 Vigo (Spain)
E-mail: lorenzo@uvigo.es

[b] Dr. D. Aranda,+ Dr. F. Santoro
Istituto di Chimica dei Composti Organometallici
Consiglio Nazionale delle Ricerche
Via Madonna del Piano 10, 50019 Sesto Fiorentino, Pisa (Italy)
E-mail: fabrizio.santoro@pi.iccom.cnr.it

[c] Dr. M. Talavera
Department of Chemistry
Humboldt Universität zu Berlin
Brook-Taylor-Strasse 2, 12489 Berlin (Germany)

[d] Dr. B. Covelo
CACTI (Centro de Apoyo Científico-Tecnológico a la Investigación)
Universidad de Vigo
Campus Universitario, 36310 Vigo (Spain)

[e] Prof. Á. Peña-Gallego
Departamento de Química Física
Universidad de Vigo
Campus Universitario, 36310 Vigo (Spain)
E-mail: mpena@uvigo.es

[+] A. O. and D. A. contributed equally to this manuscript.

ChemPlusChem

Research Article
doi.org/10.1002/cplu.202100554

Chemistry Europe
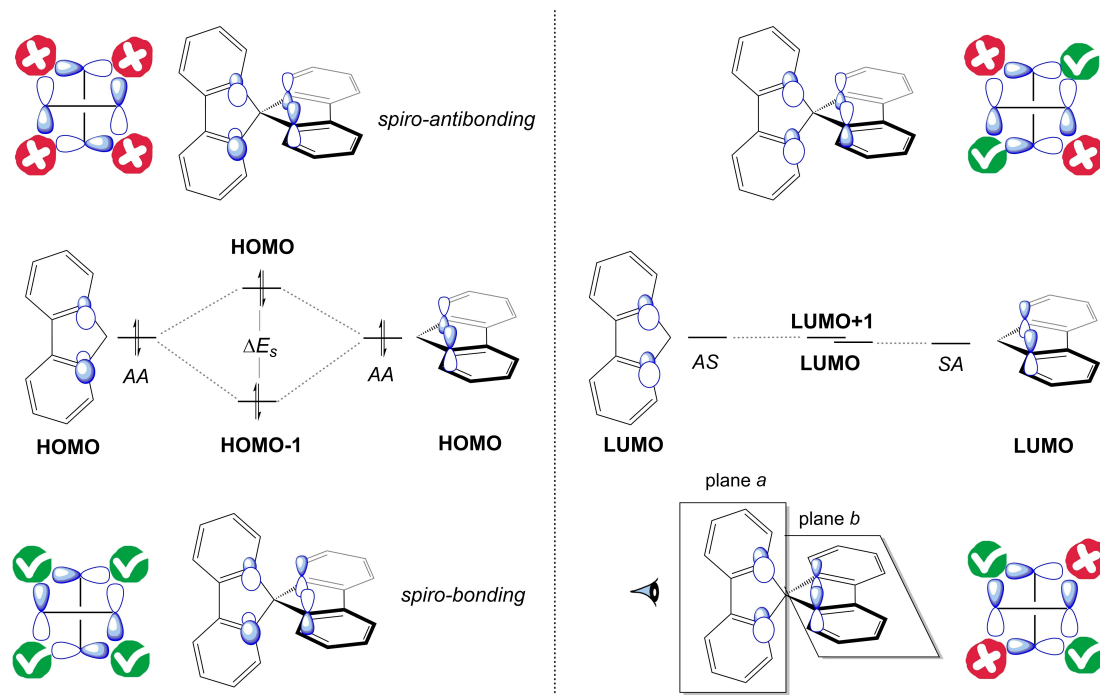European Chemical
Societies Publishing

Figure 1. Representation of the energy diagram for spiroconjugative interactions in HOMO/HOMO-1 and degenerate LUMO/LUMO + 1 in 9,9-spirobifluorene and Newman projections of the corresponding MOs. For *p* orbitals of carbon atoms directly bound to the spiro center, symmetry denotations are given for planes a and b, respectively. The fully antisymmetric combination is denoted as AA, whereas antisymmetric/symmetric arrangements are expressed by SA or AS. Red crosses and green checks stand for mismatched and matched signs between the lobes of the *p* orbitals, respectively.

consequence of spiroconjugative interactions, whereas mixed arrangements (AS or SA) of the *p* orbitals prevent spiro-splitting of LUMO/LUMO + 1 pair.[3,4,7] This phenomenon was first demonstrated by Schweig and co-workers via photoelectron spectroscopy measurements.[5] The impact of spiroconjugation on the optical properties of model SBFs was later discussed in terms of exciton coupling[25] and charge-resonance state models.[26] Nevertheless, there has been little discussion on integrating spiroconjugation as a key factor in the design of functional SBF-based materials, limiting the possibilities for their high-performance.

The cross-shaped geometry featured by SBFs offers axial chirality upon asymmetric substitution. This requires, at least, two (identical or different) substituents placed in the perpendicular fluorene units.[8,27–29] 2-Substituted SBFs are the most studied regioisomers due to their synthetic availability, as well as ability to extend *π*-conjugation.[29,30] We theoretically proposed that SBFs can serve as suitable building blocks for the construction of chiroptical systems (Scheme 1).[31] Thereafter, we synthesized all-carbon double helices and flexible shape-persistent macrocycles,[32] as well as conformationally locked trimeric cyclooligomers with helical MOs.[33] Furthermore, we prepared the first metallaaromatic SBF compound, the absorption spectrum of which exhibited a strong red-shift with respect to the bare SBF.[34] More recently, we have functionalized chiral SBFs with anchoring groups to enable surface functionalization (Scheme 1).[35] Poriel and co-workers have also documented that electronic and steric effects play a critical role in the optical properties of SBF derivatives.[36] Yet, in the literature there are
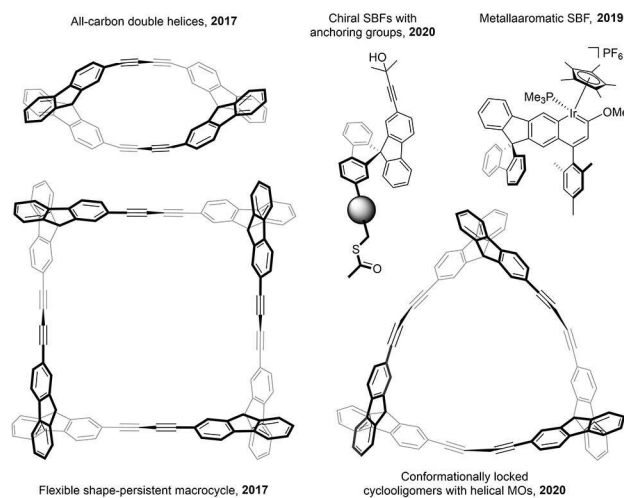

Scheme 1. Chiral spirobifluorenes previously developed in our group.

only very limited studies on structure-spiroconjugation relationships in SBFs.[7] In this work, we establish a firm relationship between spiroconjugation and chemical reactivity and we investigate theoretically its connection with optical properties. To this end, we present the synthesis of SBFs **1a**–**2c** bearing functional groups with different electronic character. Our experimental-theoretical approach demonstrates that spiroconjugation can be turned ON and OFF via peripheral functionalization. Furthermore, we hypothesize that spiroconjugation has a direct impact on the reactivity of **1a**–**1c**, however, further work

ChemPlusChem

Research Article
doi.org/10.1002/cplu.202100554

Chemistry Europe
European Chemical
Societies Publishing

to certify this scheme is out of the scope of this work. Additionally, the spiroconjugated MOs present a major role in the low energy transitions, however with no apparent impact on the signature of the resulting optical and chiroptical responses of **2a**–**2c**.

Results and Discussion

Chiral racemic SBFs **1a**–**2c** were all prepared under the same Pd/Cu-catalyzed Sonogashira conditions. First, commercially available aryl bromides were transformed into the corresponding acetylenes by two-step cross-coupling and deprotection reactions using well-known procedures (Scheme 2, for further details see the Supporting Information).[37,38] Next, Sonogashira reaction between commercially available phenyl acetylene **a** and (±)-**3** using [Pd(PPh$_3$)$_2$Cl$_2$], CuI, and Et$_3$N in DMF at 80 °C furnished monosubstituted (±)-**1a** and disubstituted (±)-**2a** in 37% and 24% yield, respectively. Under the same reaction conditions, the reaction of (±)-**3** with the electron-withdrawing nitrophenyl alkyne **b** led to (±)-**1b** and (±)-**2b** in 26% and 7% yield, respectively. Electron-donating dimethylaniline acetylene **c**, on the other hand, drove to monocoupled (±)-**1c** in 48% yield and much less to dicoupled (±)-**2c** (8%). The electron-donating ability of the amino group hence dramatically deactivates the C–Br bond of the neighboring fluorene moiety in (±)-**1c**. For monofunctionalized (±)-**1a** and (±)-**1b**, however, the second alkynylation was not significantly affected by peripheral functionalization and this was rationalized by weak through-space orbital interactions. Additionally, Sonogashira reactions of nitro-bearing compound (±)-**1b** and dimethylamino-bearing compound (±)-**1c** with dimethylaniline acetylene **c** were also performed using the same Pd/Cu-catalyzed protocol. While the cross-coupling with (±)-**1b** proceeded in 53% yield of (±)-**2bc**, that of (±)-**1c** provided (±)-**2c** only in 26% yield. Taking into account that transmetalation is generally the rate-limiting step for Sonogashira reaction and oxidative addition may undertake this role in processes involving electron-rich aryl bromides,[39] all these findings validate the deactivation of the C–Br bond in SBFs by electron-rich neighboring fluorenes toward Sonogashira reaction.
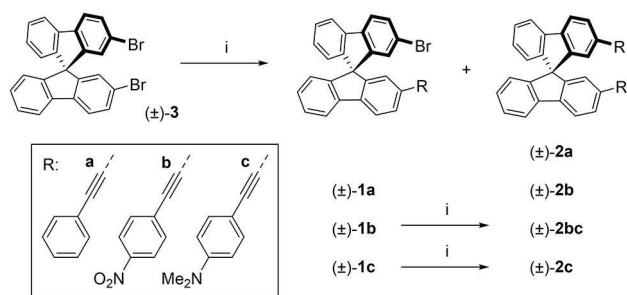
Theoretical calculations have been used to examine through-space orbital interactions in numerous spiro systems.[1,3,6,8,40] Recently, Amaya et al. have performed a comprehensive DFT study over chiral cyclic [*n*]spirobifluorenylenes and established even-odd effects for systems with multiple bifluorenyl units.[7] In the present study the occupied MOs of monofunctionalized SBFs (*P*)-**1a**, (*P*)-**1b**, and (*P*)-**1c** were computed at the CAM-B3LYP/6-31G(d,p) level to determine whether the experimental results obtained from the Sonogashira cross-coupling can be justified by through-space orbital interactions. Notably, (*P*)-**1c** presents the strongest spiroconjugative interactions in terms of the *p* orbital symmetry around the tetrahedral carbon atom (Figure 2). The energy splitting between spiro-antibonding HOMO-1 and spiro-bonding HOMO-2 is calculated as 0.22 eV, very similar to those of bare SBF or (*P*)-**3**. The electron density of HOMO in (*P*)-**1c** is also mainly distributed over the amino functionalized fluorene rather than the bromo-fluorene subunit, and therefore it does not participate in the phenomenon of spiroconjugation. When analyzing the occupied MOs of (*P*)-**1a** and (*P*)-**1b** at the same level of theory, no significant spiroconjugative interactions were found (see Figures S46–S48 in the Supporting Information). Consequently, HOMO-1 and HOMO-2 of (*P*)-**1c** deactivate the electrophilic position of this particular compound by the electron-donating ability of the amino group in Sonogashira cross-coupling: once the first coupling of amino alkyne to (±)-**3** has been achieved, spiroconjugative effects become operative in (±)-**1c** (ON) and diminish its reactivity toward a second Sonogashira coupling, yet its implication for (±)-**1a** and (±)-**1b** is negligible (OFF). Overall, these results let us postulate that spiroconjugation plays an important role in the reactivity of (±)-**1c**, however, further kinetic studies would be necessary to verify this assumption (Figure 3).

Single crystals of (±)-**1a**, (±)-**1c**, (±)-**2a**, (±)-**2b**, and (±)-**2bc**, suitable for X-ray diffraction analysis, were grown by slow evaporation technique using mixtures of *n*-hexane/CH$_2$Cl$_2$, CH$_2$Cl$_2$/MeOH, or *n*-hexane/EtOAc (Deposition Number(s) (±)-**1a** (CCDC-2067406), (±)-**1c** (CCDC-2067407), (±)-**2a** (CCDC-2067408), (±)-**2b** (CCDC-2067409), and (±)-**2bc** (CCDC-2067410), contain(s) the supplementary crystallographic data for this paper. These data are provided free of charge by the joint Cambridge Crystallographic Data Centre and Fachinformationszentrum Karlsruhe Access Structures service, for more details, see the Supporting Information). SBFs (±)-**1c**, (±)-**2b**, and (±)-**2bc** crystallized in an achiral triclinic *P*-1 space group,

Scheme 2. Synthesis of racemic SBFs **1a**–**1c** and **2a**–**2c** from **3**, as well as **2bc** and **2c** from **1b** and **1c**, respectively. Reagents and conditions: i) [Pd(PPh$_3$)$_2$Cl$_2$], CuI, Et$_3$N, DMF, 80 °C, 24 h. DMF: *N*,*N*-dimethylformamide.
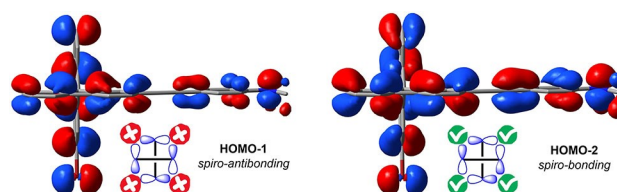

Figure 2. Representation of HOMO-1 (left) and HOMO-2 (right) of monofunctionalized (*P*)-**1c** at the CAM-B3LYP/6-31G(d,p) level of theory. Kohn-Sham molecular orbitals are shown with an isosurface value of 0.02 electrons/bohr^3.
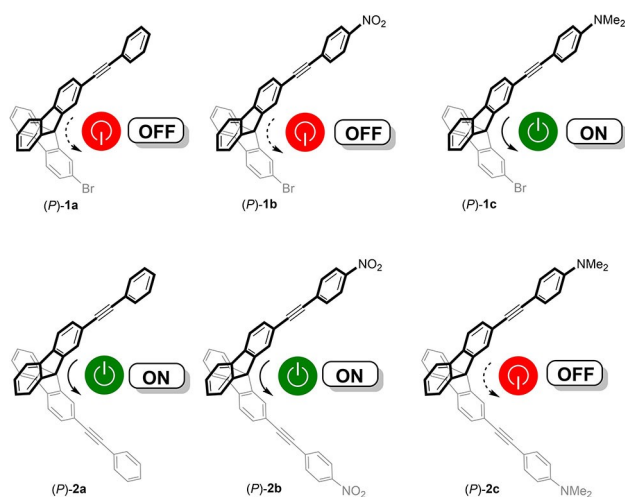
ChemPlusChem

Research Article
doi.org/10.1002/cplu.202100554

Chemistry Europe
European Chemical
Societies Publishing

Figure 3. ON/OFF modulation of spiroconjugation through peripheral functionalization in spirobifluorenes **2a–2c**.

yet (±)-**1a** and (±)-**2a** crystallized in the chiral monoclinic P-2_1 space group by which spontaneous enantiomeric resolution occurred only in the crystallization of difunctionalized (±)-**2a**. The asymmetric units of homochiral (P^*)-**2a** and (±)-**2bc** comprised one molecule of the SBF derivative, whereas two molecules of the SBF derivative together with molecules of crystallization solvent were encountered for the others. For all structures, the bond lengths and angles of the constituent molecules were comparable with other compounds bearing the SBF core.[41–43] While the formation of supramolecular assemblies by C−Br⋯π, C−H⋯π, or non-classical hydrogen bonding including C−H⋯O interactions were observed for all the structures, none of these derivatives showed π-π stacking interactions. Such behavior is characteristic of SBF derivatives due to the perpendicular linkage between two fluorene units.[16]

Optically active solutions of **2a** were obtained from sets of crystals dissolved in CH_2Cl_2. Enantiomeric resolution of (±)-**2b** and (±)-**2c**, on the other hand, was successfully achieved through HPLC on a chiral stationary phase (CSP). Apart from high photostability in solution, thermogravimetric analysis and differential scanning calorimetry revealed that (±)-**2a**, (±)-**2b**, (±)-**2bc**, and (±)-**2c** present thermal stability from ca. 220 °C to 500 °C under air atmosphere (for more details on the enantiomeric resolution and stability, see the Supporting Information).

Optical and chiroptical properties of the functionalized SBFs were measured in CH_2Cl_2. Figure 4 shows that the electronic circular dichroism (ECD) spectra of (P)-**2a** features three narrow positive peaks at ∼330 nm, followed by negative peaks in the 300–250 nm region; yet the UV/Vis is characterized by three narrow peaks at ∼330 nm and a very weak band at ∼260 nm. On the other hand, ECD spectra of (P)-**2b** and (P)-**2c** feature a positive band at ∼380 nm followed by two negative bands at ∼340 and ∼290 nm, corresponding to two broad bands in the UV/Vis spectra (for more information, see the Supporting Information). Prediction of UV/Vis and ECD spectra including vibronic contributions, as well as couplings between the different electronic states and the solvent inhomogeneous broad-

ening satisfactorily reproduced those observed experimentally (Figure 4, for absorption see Supporting Information). This achievement was only possible thanks to very recent methodological developments.[44,45] Briefly, we adopted a Linear Vibronic Coupling (LVC) model parametrized with CAM-B3LYP/6-31G(d) considering as reference states only the adiabatic states at the ground-state equilibrium geometry involving excitations from HOMO-1 and HOMO, to LUMO and LUMO+1, i.e the two lowest-energy states S1 and S2, which carry significant oscillator and/or rotatory strength and a pair of higher-energy states with inter-monomer charge-transfer (CT) character (see Table S5 in Supporting Information). We also estimated the solvent inhomogeneous broadening with PCM calculations (further details are given in the Supporting Information, see Table S15).[46] The good agreement with the experimental spectra allows us to assign the (P) absolute configuration for fractions exhibiting a positive sign for the lowest energy band, as expected from the exciton chirality rule,[47] and indicates that the set of bands around 330 nm in the ECD spectrum of (P)-**2a** originates from vibronic progressions. Computed spectra in Figure 4 attribute the absence of such vibronic signatures in (P)-**2b** and (P)-**2c** to the existence of a remarkable inhomogeneous solvent broadening, which is induced by a partial CT character (between the peripheral moieties and central core) of the states involved. Such CT character is remarkable in (P)-**2b** and (P)-**2c** due to the presence of functional groups with strong electron-withdrawing or electron-donating character, yet it is negligible in (P)-**2a**. The importance of vibronic and solvent broadening effects on the ECD spectra are highlighted in the Supporting Information where we report spectra computed at pure electronic level (Figure S44) or at vibronic level with only a phenomenological broadening (Figure S43). In the Supporting Information we also give additional details on the theoretical methodology applied to simulate the spectra and on the selection of the states included in the vibronic computations. An alternative picture of the effects of nonadiabatic couplings on the absorption and ECD spectra can be obtained by considering the molecule as an excitonic-type model with two interacting fluorenes including also couplings between local excitations and the corresponding CT states, involving in this case a charge exchange between the two fluorenes (since a connection between the role of such CT states and spiroconjugation has been proposed in literature).[48] Results are similar to those in Figure 4 and they are reported in the Supporting Information (Figure S44, showing that such kind of CT states play a negligible role on the spectral shapes of (P)-**2a**, (P)-**2b**, and (P)-**2c**. Finally, Supporting Information also investigates the possible impact of molecular flexibility around the spiro-carbon on the spectral shapes, concluding that it is only limited).

To understand how spiroconjugation contributes to both optical and chiroptical properties, we finally analyzed in closer detail the molecular orbitals of SBFs (P)-**2a**, (P)-**2b**, and (P)-**2c** involved in the main electronic transitions (Figure 5, for more details see the Supporting Information). The main features of the simulated ECD and UV/Vis spectra of (P)-**2a**, (P)-**2b**, and (P)-**2c** arise from S1 and S2 states, in which only HOMO and HOMO-1 have significant contributions. While the HOMO and

ChemPlusChem

Research Article
doi.org/10.1002/cplu.202100554

Chemistry Europe
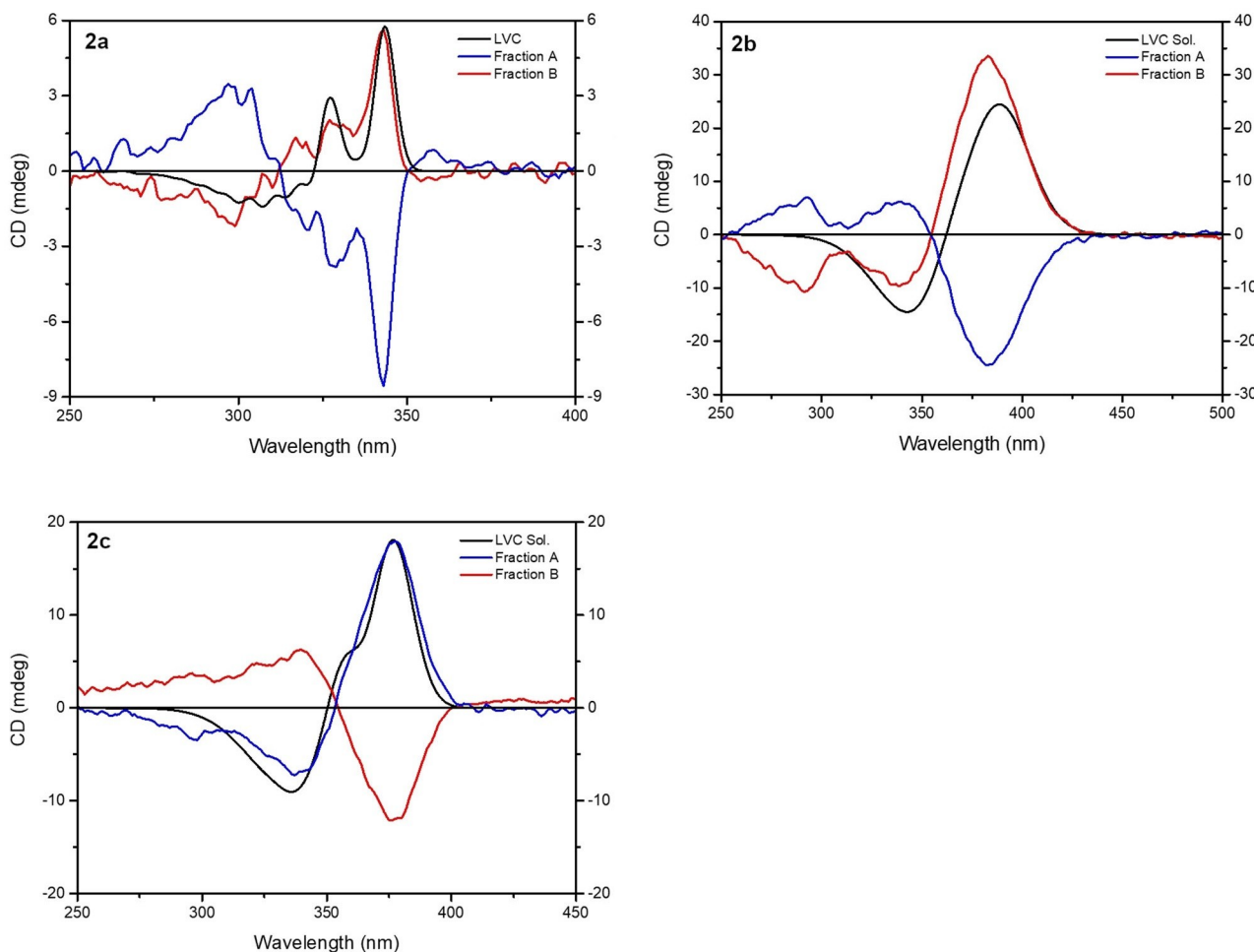European Chemical
Societies Publishing

Figure 4. Comparison of experimental and theoretical ECD spectra for **2a** (top), **2b** (middle), and **2c** (bottom). Experimental spectra of each compound were measured in CH_2Cl_2 and reported in mdeg on the left panel. Fractions A and B are depicted in blue and red, respectively. Theoretical spectra were calculated at the CAM-B3LYP/6-31G(d,p) level of theory and obtained with a nonadiabatic LVC model for the (*P*) enantiomer of each compound. For the sake of clarity, theoretical spectra of **2a**, **2b** and **2c** were red-shifted by 0.17, 0.33 and 0.30 eV for **2a**, **2b** and **2c** and the intensities were scaled by arbitrary factors. Solvent inhomogeneous broadening was introduced on the computed spectra (*P*)-**2b** and (*P*)-**2c** by convolution with a Gaussian whose half-width at half-maximum (HWHM) was determined according to Marcus's theory: of 0.13 and 0.08 eV, respectively. These spectra are indicated as "LVC Sol" in the Figure and reported in $\Delta\varepsilon$ on the right panel. The corresponding solvent broadening for (*P*)-**2a** was estimated to be negligible, and for this species we adopted a convolution with a Gaussian with HWHM = 0.04 eV to phenomenologically include all other broadening sources like thermal excitation. ("LVC" label). From these results for (*P*)-**2a**, Fraction A can be assigned to the (*P*) enantiomer. Experimental maximum *g-factor* values: 0.0002 for **2a** (343 nm), 0.001 for **2b** (383 nm) and 0.001 for **2c** (377 nm).

HOMO-1 of (*P*)-**2a** (ON) and (*P*)-**2b** (ON) showed spiro-splitting with a value of 0.10 eV and 0.14 eV, respectively, (*P*)-**2c** (OFF) does not present spiroconjugation in these MOs. Such differences are due to peripheral functionalization that increases in (*P*)-**2b** and decreases in (*P*)-**2c** the electron density (and therefore the spiro-splitting) on the carbon atoms bound to the spiro carbon. Peripheral functionalization thus controls the spiroconjugation of the MOs relevant for the main optical and chiroptical properties of SBFs, specifically: in (*P*)-**2a** (ON) and (*P*)-**2b** (ON), and **2c** (OFF) (Figure 3). Whereas such splitting does not appear to have a clear signature on the experimental spectra, it is interesting to note that the same electron-donor or acceptor properties of the functional groups affecting spiroconjugation also dictate the magnitude of the solvent inhomogeneous broadening, i.e. the key factor for distinguishing the

shape of the electronic spectra of (*P*)-**2a** with respect to those of (*P*)-**2b** and (*P*)-**2c**.

Conclusions

In summary, we have designed and synthesized robust chiral SBFs with different functionalities. Both experimental and theoretical results allow us to hypothesize that the phenomenon of spiroconjugation becomes ON for the reactivity of SBFs monosubstituted by electron donating groups. Additionally, spontaneous enantiomeric resolution and CSP-HPLC method have successfully afforded the optically active solutions of **2a**, **2b**, and **2c**. As verified by theoretical analysis, the MOs responsible for spiroconjugative interactions have an important
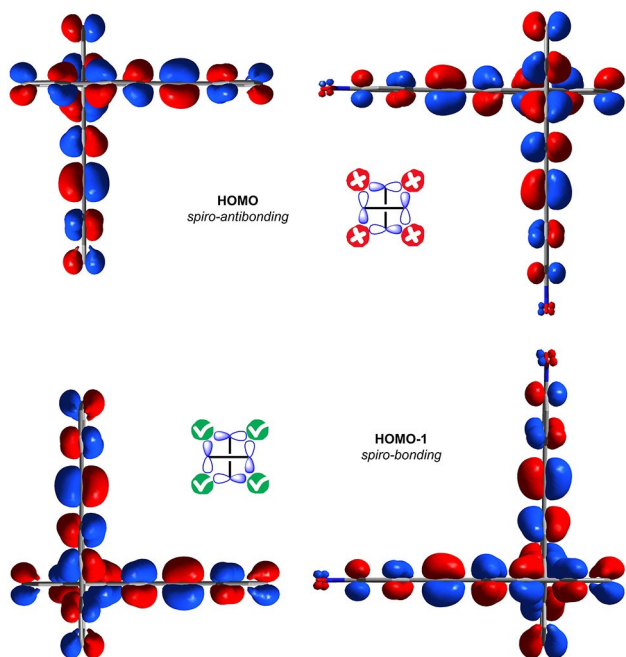
ChemPlusChem

Research Article
doi.org/10.1002/cplu.202100554

Chemistry
Europe

European Chemical
Societies Publishing

Figure 5. Representation of HOMO (top) and HOMO-1 (bottom) of (P)-**2 a** (left) and (P)-**2 b** (right) at the CAM-B3LYP/6-31G(d,p) level of theory. Kohn-Sham molecular orbitals are shown with an isosurface value of 0.02 electrons/bohr.[3]

participation (ON) on the electronic transitions responsible of the main features of the ECD and UV/Vis spectra of **2 a** and **2 b**, but this does not translate into remarkably different splitting of the electronic states, so that differences in the final optical response are more connected with the CT character of the transitions (between the functional groups and the central core). Overall, the present work assesses the impact of spiroconjugation on the reactivity and optical properties controlled by peripheral functionalization. We believe that our findings will provide a springboard for the development of tailored SBFs suitable for chiroptical and spintronic applications not only by controlling their synthesis, but also by modulating their optoelectronic properties.[49,50] We are currently evaluating SBFs with other functional groups to gain a deeper understanding in this phenomenon.

Conflict of Interest

The authors declare no conflict of interest.

Data Availability Statement

The data that support the findings of this study are available in the supplementary material of this article.

[1] H. E. Simmons, T. Fukunaga, *J. Am. Chem. Soc.* **1967**, *89*, 5208–5215.
[2] R. Hoffmann, A. Imamura, G. D. Zeiss, *J. Am. Chem. Soc.* **1967**, *89*, 5215–5220.
[3] H. Dürr, R. Gleiter, *Angew. Chem. Int. Ed.* **1978**, *17*, 559–569; *Angew. Chem.* **1978**, *90*, 591–601.
[4] R. Gleiter, G. Haberhauer, in *Aromat. Other Conjug. Eff.* (Eds.: R. Gleiter, G. Haberhauer), Wiley-VCH, Weinheim, Germany, **2012**, pp. 133–216.
[5] A. Schweig, U. Weidner, D. Hellwinkel, W. Krapp, *Angew. Chem. Int. Ed.* **1973**, *12*, 310–311; *Angew. Chem.* **1973**, *85*, 360–361.
[6] J. Wilbuer, G. Schnakenburg, B. Esser, *Eur. J. Org. Chem.* **2016**, *2016*, 2404–2412.
[7] K. Zhu, K. Kamochi, T. Kodama, M. Tobisu, T. Amaya, *Chem. Sci.* **2020**, *11*, 9604–9610.
[8] J. Oniki, T. Moriuchi, K. Kamochi, M. Tobisu, T. Amaya, *J. Am. Chem. Soc.* **2019**, *141*, 18238–18245.
[9] M. Tsuji, T. Ohwada, K. Shudo, *Tetrahedron Lett.* **1998**, *39*, 403–406.
[10] H. Igarashi, S. Sakamoto, K. Yamaguchi, T. Ohwada, *Tetrahedron Lett.* **2001**, *42*, 5257–5260.
[11] P. Maslak, S. Varadarajan, J. D. Burkey, *J. Org. Chem.* **1999**, *64*, 8201–8209.
[12] A. Schweig, U. Weidner, R. K. Hill, D. A. Cullison, *J. Am. Chem. Soc.* **1973**, *95*, 5426–5427.
[13] C. Batich, E. Heilbronner, E. Rommel, M. F. Semmelhack, J. S. Foos, *J. Am. Chem. Soc.* **1974**, *96*, 7662–7668.
[14] A. D. Baker, M. A. Brisk, T. J. Venanzi, Y. S. Kwon, S. Sadka, D. C. Liotta, *Tetrahedron Lett.* **1976**, *17*, 3415–3418.
[15] S. Smolinski, M. Balazy, H. Iwamura, T. Sugawara, Y. Kawada, M. Iwamura, *Bull. Chem. Soc. Jpn.* **1982**, *55*, 1106–1111.
[16] T. P. I. Saragi, T. Spehr, A. Siebert, T. Fuhrmann-lieker, J. Salbeck, *Chem. Rev.* **2007**, *107*, 1011–1065.
[17] M. Valášek, K. Edelmann, L. Gerhard, O. Fuhr, M. Lukas, M. Mayor, *J. Org. Chem.* **2014**, *79*, 7342–7357.
[18] Q. Wang, F. Lucas, C. Quinton, Y. K. Qu, J. Rault-Berthelot, O. Jeannin, S. Y. Yang, F. C. Kong, S. Kumar, L. S. Liao, C. Poriel, Z. Q. Jiang, *Chem. Sci.* **2020**, *11*, 4887–4894.
[19] Y. Wu, D. Wu, H. Zhao, J. Li, X. Li, Z. Wang, H. Wang, F. Zhu, B. Xu, *RSC Adv.* **2019**, *9*, 22176–22184.
[20] Y. Wu, J. Li, W. Liang, J. Yang, J. Sun, H. Wang, X. Liu, B. Xu, W. Huang, *New J. Chem.* **2015**, *39*, 5977–5983.
[21] Y. Ferrand, C. Poriel, P. Le Maux, J. Rault-Berthelot, G. Simonneaux, *Tetrahedron: Asymmetry* **2005**, *16*, 1463–1472.
[22] M. Wang, X. Wei, W. Zhang, H. Zhao, Y. Wu, Y. Miao, H. Wang, B. Xu, *J. Solid State Chem.* **2021**, *298*, 122122.
[23] D. Becker, N. Konnertz, M. Böhning, J. Schmidt, A. Thomas, *Chem. Mater.* **2016**, *28*, 8523–8529.
[24] Y. Wu, J. Li, W. Liang, J. Yang, J. Sun, H. Wang, X. Liu, B. Xu, W. Huang, *RSC Adv.* **2015**, *5*, 49662–49670.
[25] J. Sagiv, A. Yogev, Y. Mazur, *J. Am. Chem. Soc.* **1977**, *99*, 6861–6869.
[26] J. Spanget-Larsen, R. Gleiter, R. Haider, *Helv. Chim. Acta* **1983**, *66*, 1441–1455.

[27] J. H. Xie, Q. L. Zhou, *Acc. Chem. Res.* **2008**, *41*, 581–593.

[28] H. Hamada, Y. Itabashi, R. Shang, E. Nakamura, *J. Am. Chem. Soc.* **2020**, *142*, 2059–2067.

[29] C. Poriel, J. Rault-Berthelot, L. J. Sicard, *Chem. Commun.* **2019**, *55*, 14238–14254.

[30] X. Liu, Y. Zhang, X. Fei, M. Fung, J. Fan, *Chem. A Eur. J.* **2019**, *25*, 6788–6796.

[31] S. Castro-Fernández, M. M. Cid, C. S. López, J. L. Alonso-Gómez, *J. Phys. Chem. A* **2015**, *119*, 1747–1753.

[32] S. Castro-Fernández, R. Yang, A. P. García, I. L. Garzón, H. Xu, A. G. Petrovic, J. L. Alonso-Gómez, *Chem. Eur. J.* **2017**, *23*, 11747–11751.

[33] A. Ozcelik, D. Aranda, S. Gil-Guerrero, X. A. Pola-Otero, M. Talavera, L. Wang, S. K. Behera, J. Gierschner, Á. Peña-Gallego, F. Santoro, R. Pereira-Cameselle, J. L. Alonso-Gómez, *Chem. Eur. J.* **2020**, *26*, 17342–17349.

[34] V. C. Arias-Coronado, R. Pereira-Cameselle, A. Ozcelik, M. Talavera, Á. Peña-Gallego, J. L. Alonso-Gómez, S. Bolaño, *Chem. A Eur. J.* **2019**, *22*, 13496–13499.

[35] A. Ozcelik, M. de los Á Peña-Gallego, R. Pereira-Cameselle, J. L. Alonso-Gómez, *Chirality* **2020**, *32*, 464–473.

[36] L. Sicard, C. Quinton, J.-D. Peltier, D. Tondelier, B. Geffroy, U. Biapo, R. Métivier, O. Jeannin, J. Rault-Berthelot, C. Poriel, *Chem. Eur. J.* **2017**, *23*, 7719–7727.

[37] N. Gulia, B. Pigulski, S. Szafert, *Organometallics* **2015**, *34*, 673–682.

[38] C. Li, C. Gao, J. Lan, J. You, G. Gao, *Org. Biomol. Chem.* **2014**, *12*, 9524–9527.

[39] R. Chinchilla, C. Nájera, *Chem. Rev.* **2007**, *107*, 874–922.

[40] D. Meng, R. Wang, J. B. Lin, J. L. Yang, S. Nuryyeva, Y. Lin, S. Yuan, Z. Wang, E. Zhang, C. Xiao, D. Zhu, L. Jiang, Y. Zhao, Z. Li, C. Zhu, K. N. Houk, Y. Yang, *Adv. Mater.* **2021**, *33*, 2006120.

[41] R. E. Douthwaite, A. Taylor, A. C. Whitwood, *Acta Crystallogr. Sect. C* **2005**, *61*, o328–o331.

[42] L. R. Nassimbeni, N. B. Báthori, L. D. Patel, H. Su, E. Weber, *Chem. Commun.* **2015**, *51*, 3627–3629.

[43] Y. Nishii, M. Ikeda, Y. Hayashi, S. Kawauchi, M. Miura, *J. Am. Chem. Soc.* **2020**, *142*, 1621–1629.

[44] M. Y. Jouybari, Y. Liu, R. Improta, F. Santoro, *J. Chem. Theory Comput.* **2020**, *16*, 5792–5808.

[45] D. Aranda, F. Santoro, *J. Chem. Theory Comput.* **2021**, *17*, 1691–1700.

[46] R. A. Marcus, *J. Phys. Chem.* **1989**, *93*, 3078–3086.

[47] N. Harada, K. Nakanishi, *Acc. Chem. Res.* **1972**, *5*, 257–263.

[48] K. Shingu, H. Kuritani, A. Kato, S. Imajo, *Tetrahedron Lett.* **1980**, *21*, 3997–4000.

[49] M. S. Zöllner, A. Saghatchi, V. Mujica, C. Herrmann, *J. Chem. Theory Comput.* **2020**, *16*, 7357–7371.

[50] W. Mtangi, F. Tassinari, K. Vankayala, A. Vargas Jentzsch, B. Adelizzi, A. R. A. Palmans, C. Fontanesi, E. W. Meijer, R. Naaman, *J. Am. Chem. Soc.* **2017**, *139*, 2794–2798.